Atomic scale friction and adhesion properties of quasicrystal surfaces

2008 J. Phys.: Condens. Matter 20 314012

(http://iopscience.iop.org/0953-8984/20/31/314012)

IOP Publishing Journal of Physics: Condensed Matter

J. Phys.: Condens. Matter **20** (2008) 314012 (14pp) doi:10.1088/0953-8984/20/31/314012

Atomic scale friction and adhesion properties of quasicrystal surfaces

Jeong Young Park[1,2,4] **and P A Thiel**[3]

[1] Lawrence Berkeley National Laboratory, University of California, Berkeley, CA 94720, USA
[2] Department of Chemistry, University of California, Berkeley, CA 94720, USA
[3] Ames Laboratory and Department of Chemistry, Iowa State University, Ames, IA 50011, USA

E-mail: jypark@lbl.gov

Received 18 March 2008, in final form 2 May 2008
Published 11 July 2008
Online at stacks.iop.org/JPhysCM/20/314012

Abstract

In this paper, we highlight recent studies of the atomic scale friction and adhesion properties of quasicrystals. We review tribological studies carried out in different mechanical regimes (elastic and inelastic) and at different length scales (macroscale and nanoscale). We address the role of the surface oxide and the nature of mechanical contact in determining friction and adhesion properties. We discuss the relationship between the aperiodic atomic structure of quasicrystals and their low friction, for both elastic and inelastic regimes.

(Some figures in this article are in colour only in the electronic version)

1. Introduction

Interfaces between quasicrystals and other materials can be static or dynamic. The present paper deals with dynamic interfaces in which the two respective bulk samples are in relative motion. The topic is particularly important because interfaces between quasicrystals and other materials are reported to exhibit low coefficients of friction and low adhesion. This is one of the most intriguing, and potentially useful, features of these alloys.

The anomalously low coefficients of friction were first discovered by Dubois *et al* who measured the frictional properties of quasicrystals when sliding against diamond and steel [1–3]. They reported that the 'friction coefficient is less than half that of the aluminum-based substrates studied in the present paper and as good as that of a low-carbon steel'. There have been a number of experimental and theoretical efforts to elucidate this effect since then. Tribological measurements have been carried out on quasicrystalline surfaces with atomic force microscopy [4–8], and also with more conventional tribometry [9–12]. Understanding the relation between the low friction on the quasicrystal surface and its exotic atomic structure is important in order to unravel the basic physics/chemistry of friction and to facilitate practical applications such as nanoscale moving parts.

The problem, however, is that friction is a complex process. When inelastic deformation occurs during sliding, the possible channels for energy dissipation include breaking of surface chemical bonds, generation of point defects, interactions with wear debris [13], phase transformations near the sliding track [14], creation of dislocations and phasons [15, 16] and (in crystalline materials) propagation of slip planes in specific crystallographic directions. When deformation is elastic, on the other hand, there are mainly two possibilities, namely, excitation of phonons or electron–hole pairs. Hence, elastic deformation presents a much simpler—albeit less 'realistic'—context in which to try to understand friction. Until recently, all measurements of friction on quasicrystals had been done under conditions where some inelastic deformation took place.

Various explanations for low friction on quasicrystals have been put forth. It has not been easy to determine which is correct, and it is possible that different explanations prevail at different interfaces and under different sliding conditions. Singer *et al* proposed that the oxide (which is present during friction in air) serves as a third-body lubricant, and that this lubricant is especially effective because the oxide readily delaminates from the quasicrystal [13]. Mancinelli *et al* suggested that the high hardness of the quasicrystal is responsible, based upon an inverse relationship between hardness and friction coefficients for a series of five clean metals (including a quasicrystal) [17]. Incommensurability at the sliding interface was proposed as well, the idea being

[4] Author to whom any correspondence should be addressed.

that this could inhibit phonon excitation [18, 19]. Some studies show no tribological difference between quasicrystals and similar crystalline materials [12].

Clearly, it is valuable to design experiments that are sufficiently simple and focused to differentiate among the myriad possibilities. In this vein, Dubois *et al* compared a range of quasicrystals and crystalline materials of related composition. They measured friction coefficients using tribometry and correlated the friction coefficient with the electronic structure of the material [10, 20, 21], concluding that electronic structure dominates atomic structure in importance [22–25]. Another approach, which is highlighted in this review, is to use scanning probe techniques because they allow access to both elastic and inelastic contacts, and because the contact mechanics can be interpreted within the framework of relatively straightforward models. In any approach, it is important to note that friction coefficient or friction force is not a fundamental property of a single material, but rather a property of the combination of materials that comprise the sliding interface, plus its environment and mechanical characteristics. Therefore, comparisons between different systems are necessary, but are most enlightening when the number of variables is minimized.

In this paper, we highlight recent studies of adhesion and friction on quasicrystal surfaces using nanoscale techniques, but we make some comparisons with techniques that yield macroscopic information. We address the influence of the surface atomic structure, and the roles of elastic/inelastic deformation and of oxidation on the tribological and mechanical properties of quasicrystal surfaces.

Sections 2–4 provide background on experimental tools for tribology, the tribological environment and the surface oxide, and models for contact mechanics. Sections 5–8 use this information to analyze experimental data concerning adhesion and friction. Results from different experiments are compared and rationalized when possible. Finally, in section 9 we provide some thoughts about the role of elementary properties of quasicrystals in friction.

2. Experimental tools for tribology

Various techniques have been used to elucidate the friction properties of quasicrystalline materials [14, 22–31]. In earlier studies, macroscopic techniques such as tribometer and pin-on-disc were utilized to reveal low friction on quasicrystalline materials. The atomic and friction force microscope (AFM/FFM) [32] has been used more recently to address the atomic scale origin of friction due to the nanometer size of the tip–sample contact area. The FFM combined with other scanning probe modes revealed important interfacial effects at the nanoscale, such as adhesion, friction, wear and lubrication, conductance, chemical reactivity and tribochemistry [33–36]. Together with the AFM/FFM techniques, surface force apparatus [37, 38] and quartz–crystal microbalance [39] techniques have been widely used to study the new physics of nanometer scale tribology such as atomic scale stick–slip and confinement of liquid films. Here, we discuss two tribological techniques, pin-on-disc and AFM/FFM, that yield tribological data at the macroscale and nanoscale, respectively.

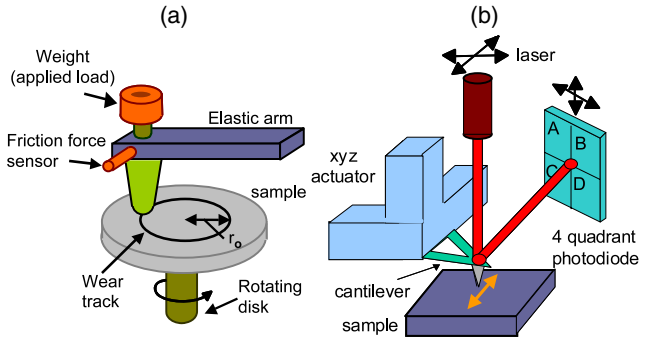

Figure 1. Schematic of (a) pin-on-disc tribometer and (b) atomic force microscope (AFM).

2.1. Pin-on-disc

A schematic of the pin-on-disc measurement is shown in figure 1(a). The apparatus consists of a 'pin' in contact with a rotating disc. In a typical pin-on-disc experiment, the coefficient of friction is continuously monitored by measuring friction force with force sensors while the fixed load is applied to the pin–sample contact [14, 23]. As wear occurs, the friction coefficient changes due to chemical interactions between the pin and the surface [40]. The presence of wear can be confirmed by measuring the profile of the resulting wear track. If the sample surface is not aligned perfectly horizontally, the pin (when in contact with the sample) oscillates along a vertical direction by a distance of a few micrometers with a period of $2\pi r_0$, where r_0 is the radius of the track.

2.2. Atomic force microscopy and friction force microscopy

In AFM, a sharp tip is brought into contact with a surface, which causes normal bending (z deflection) of the cantilever supporting the tip (figure 1(b)). If the tip is then shifted with respect to the sample (or vice versa), the cantilever is also twisted. The two deformations (lever bending and lever twisting) can be detected by a laser beam, which is reflected from the rear of the cantilever into a four-quadrant photodetector. The normal force acting on the cantilever can be deduced from the normal signals acquired with the photodetector ((A + B)–(C + D) in figure 1(b)), provided that the spring constants of the cantilever and the sensitivity of the photodetector are known.

The adhesion force can be obtained by measuring the force–distance curve or 'approach–retraction curve', as shown in figure 2(a). The approach curve is the plot of the vertical cantilever bending versus the displacement of the rear end of the cantilever basis. During retraction of the AFM probe, at point a, the probe snaps out of contact with the surface. At this point, the tensile load equals the adhesion force of the tip–sample junction. Thus, the difference in force between a and b (free position) is attributed to the adhesion force [33, 41]. Friction is measured by sensing the torsional responses of a

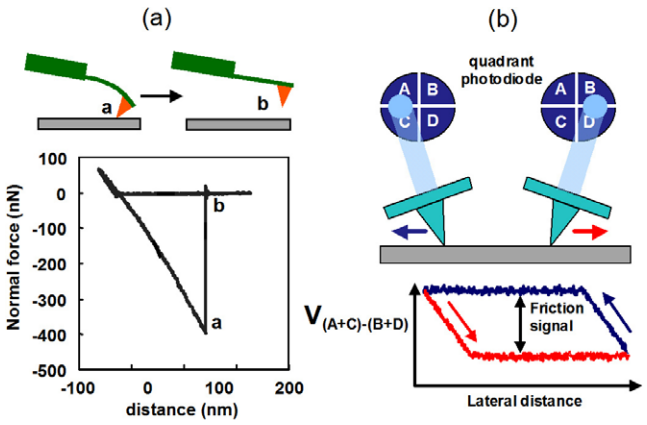

Figure 2. (a) Schematic of adhesion measurement. The force–distance curve was measured on the clean twofold Al–Ni–Co quasicrystal surface. (b) Schematic of friction measurement in AFM/FFM.

cantilever that is in contact with the surface. The torsional response of the cantilever can be deduced from the lateral signals acquired with the photodetector ((A + C)–(B + D) in figure 1(b)). As the tip scans over the track on the surface, the lateral signal ($V_{(A+C)-(B+D)}$) varies, depending on the scanning direction. Figure 2(b) shows a schematic of friction measurement and the friction loop for a uniform surface. At the beginning of the scanning, the tip sticks on the surface because of stiction (static friction) and the lateral signal changes linearly with lateral displacement (x) until the tip slides over the surface. As the tip starts sliding (in the regime of dynamic friction), the lateral signal becomes constant. The friction signal is simply the 'gap' between lateral signals of tracing and retracing, as shown in figure 2(b).

Quantitative measurements of adhesion and friction forces require knowledge of the spring constants of normal bending and lateral twisting. These parameters have been calculated based on simple beam geometry. For a rectangular narrow cantilever, the spring constant for the normal bending (k_n) and twisting (k_l) are given by [42]

$$k_n = \frac{Ewt^3}{4l^3} \tag{1}$$

$$k_l = \frac{Gwt^3}{3lh^2} \tag{2}$$

where E and G are the Young's and shear moduli, w and t are the width and thickness of the cantilever, l is the length of the cantilever from the base to the tip and h is the height of the tip. These calculated spring constants, however, have large uncertainties associated with variations in the cantilever geometry. Another way of obtaining the cantilever normal spring constant is the resonance-damping method of Sader *et al* [43]. The lateral force can be determined in situ with the wedge method of Ogletree *et al* [44].

In our own AFM experiments, topography was measured via contact AFM, using normal force for feedback. Friction force could be measured simultaneously. A cantilever coated with about 50 nm of titanium nitride, with a spring constant of 2.5 N m^{-1}, was used. Calibration of the cantilever spring constant and the lateral force was carried out as described above [43, 44]. The tip radius, R, can be determined by electron microscopy. In our experiments, the value of R after contact measurement is 100–200 nm.

3. The tribological environment and the surface oxide

Tribological measurements on Al-based quasicrystals have been carried out in air, in high vacuum (HV) and in ultrahigh vacuum (UHV). In air and at room temperature, an Al-rich oxide skin is present. Hence, tribological measurements in air, or on samples that have been exposed to air, always take place in the presence of this oxide. The advantage of working in vacuum is that the oxide can be removed, and its re-growth is hindered or prevented completely—depending upon the level of the vacuum—on the timescale of experiments. In HV, the pressure can be low enough that oxidation is limited on the timescale of successive passes of the pin on a track (cf figure 1), allowing friction measurements to be made in the presence of little or no oxide.

UHV provides an environment in which oxidation does not occur to a significant extent over periods of several hours, at least. The preparation of a clean surface in UHV typically consists of ion etching at room temperature, followed by annealing. Subsequent characterization is commonly carried out by techniques such as low energy electron diffraction (LEED), Auger electron spectroscopy (AES) and scanning tunneling microscopy (STM). Clean surfaces are often found to be bulk-terminated, within the limits of uncertainty of the analysis technique(s) [45–48].

The oxide that develops in air is somewhat complex and variable. At room temperature it does not exhibit long-range order [49], but at 700 K it does [50]. Its thickness has been reported as 2–6 nm following exposure at room temperature, with values at the upper end of the range requiring high relative humidity [51–56]. (Much thinner oxides form under typical conditions of UHV oxidation [52].) Furthermore, although most of the oxide forms instantaneously upon exposure to air, the oxide can evolve over periods of hundreds of hours. This long-term aging was first discovered in studies of pure Al [57, 58], but analogous behavior has been found in studies of an Al–Cr–Fe approximant [59]. The aging process strongly affects electrochemical properties of the oxide [59], and in section 5 we will show that it also affects tribological properties.

The oxide in air consists of three layers, as shown in figure 3 [57–59]. Adjacent to the metal is a layer of (mainly) amorphous aluminum oxide whose thickness is constant with time. Above this is a layer of amorphous aluminum oxy-hydroxides, and above that is a thin layer with high carbon content. The thicknesses of the latter two layers increase slowly with time over a period of hundreds of hours. Based on x-ray scattering, for instance, the thickness of the middle layer—the amorphous aluminum oxy-hydroxide layer—on an Al–Cr–Fe approximant has been reported to increase by about 15%, from 3.1 to 3.6 nm, over a period of 300 h [59]. Thus, one must conclude that the oxide that forms in air is not a single

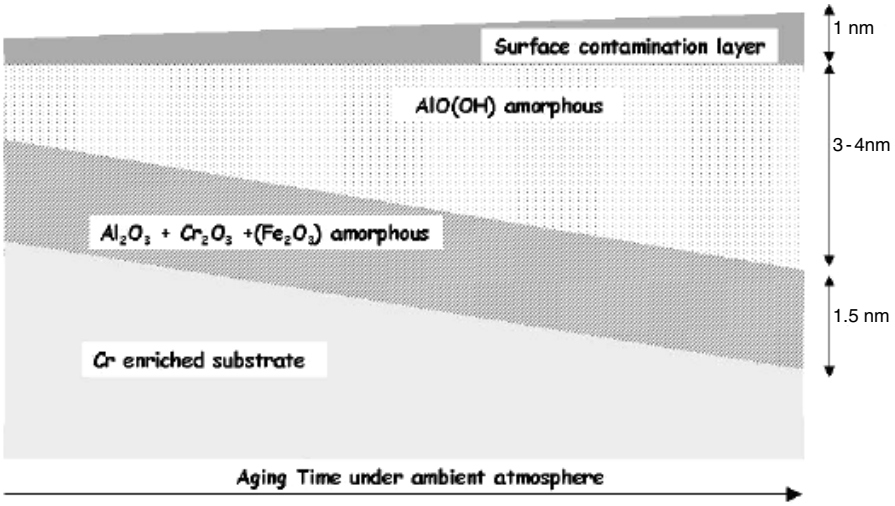

Figure 3. Model of oxide structure and composition of the oxidized surface of $Al_{65}Cr_{27}Fe_8$ during aging in air. (Reprinted with permission from the Materials Research Society [59].)

generic quantity, but rather its description depends upon the time of aging (and humidity).

Of course, the oxide that forms at a sliding interface in air should differ from that which forms on a static surface in air, largely because of local heating at the sliding interface. Previous work has shown the importance of temperature in surface oxidation of the Al-rich quasicrystals [49, 52, 60, 61]. For quasicrystals, the nature of the oxide present in tribometry studies in air has not received attention, except for one report by Singer *et al* [13]. These authors investigated a sliding interface between a tungsten carbide ball and polycrystalline Al–Cu–Fe–B using Auger electron spectroscopy. Indeed, they reported a much different composition of the oxide inside and outside of the wear track.

4. Contact mechanical models

The most basic and earliest understanding of friction was given by two principles called Amontons' laws. These state that there is a linear relation between friction force and normal force, and that the relation is independent of the apparent contact area. The ratio of friction force to normal force (load) is therefore a robust quantity, well known as the friction coefficient. These laws apply well to macroscopic interfaces, including unlubricated interfaces of metals [62] such as we will be concerned with in this paper. They are valid because friction at the macroscopic interface is due to an ensemble of microscopic asperity contacts, many of which are in a state of incipient or real plastic flow under typical tribological conditions. In this state both the friction force and the normal force are directly proportional to the contact area, so in the friction coefficient, area cancels out. It can also be shown that area is not a factor in the friction coefficient for an ensemble of asperities in elastic contact [62]. However, the assumptions upon which these derivations rest are not always valid for tribology at a single nanoscale asperity, especially at low load. Therefore, models that incorporate various levels of detail about the physical and chemical aspects of the interface are employed to understand the relationship between friction force, normal force and other parameters, in nanoscale experiments.

Three main models exist. The Hertz model is the simplest, as it incorporates purely mechanical forces. The other two, which incorporate adhesion (chemical forces), are called the Derjaguin–Müller–Toporov (DMT) [63, 64] and the Johnson–Kendall–Roberts (JKR) models [65]. These two models approximate elastic behavior in two opposite extremes. DMT describes hard and poorly adhesive materials, while JKR describes soft and adhesive materials. Any real situation is, of course, intermediate between these two extremes [66, 67]. To decide whether the behavior is closer to that predicted by DMT or JKR, an empirical non-dimensional Tabor parameter $\tau = (16R\gamma^2/9K^2z_0^3)^{1/3}$ can be used. In this formula, R is the tip radius, γ is the work of adhesion, z_0 is the equilibrium spacing of two surfaces (roughly an atomic distance) and K is the combined elastic modulus of the two materials, given by $K = 4/3[(1-\upsilon_1^2)/E_1 + (1-\upsilon_2^2)/E_2]^{-1}$, where E_1 and E_2 are their Young's moduli and υ_1 and υ_2 are the Poisson ratios. Empirically, it is found that the JKR model is a good approximation when $\tau > 5$, while DMT is more appropriate when τ is less than 0.1.

Some results for these three models, plus a model that is intermediate between DMT and JKR, are shown in figure 4. The intermediate results were calculated with the Maugis–Dugdale model for a transition parameter of 0.5 [66, 67]. The graph shows the contact area as a function of applied load for a given set of parameters. Friction force is directly proportional to contact area, so the graph also shows (qualitatively) the variation of friction force with normal load. Note that all models approach a linear relationship between normal force and friction force at high loads in figure 4, indicating that the concept of friction coefficient is applicable in this limit. Note also that, for all models except Hertz, the curves intersect the x axis at a negative value. This is because the total normal force is the sum of the adhesion force (zero in the Hertz model, non-zero in the others) plus the externally applied load. For the particular parameters indicated in figure 4, the adhesion force

Table 1. Adhesion forces and work of adhesion of decagonal Al–Ni–Co surfaces in both plastic and elastic regime against a TiN-coated tip. Work of adhesion is estimated by the DMT or JKR model, and a tip radius of 150 nm.

d-Al–Ni–Co surface	Adhesion force (μN)	Work of adhesion (J m^{-2})	Mechanical regime
Tenfold (clean) [4]	0.7 ± 0.2	0.7(DMT) $\sim$ 0.9(JKR)	Plastic
Twofold (clean) [6]	0.35 ± 0.08	0.35(DMT) $\sim$ 0.5(JKR)	
Tenfold (200 L oxygen *in situ*) [4]	0.4 ± 0.1	0.4(DMT) $\sim$ 0.5(JKR)	
Tenfold (ethylene passivated) [5]	0.07 ± 0.01	0.07(DMT) $\sim$ 0.09(JKR)	
Pt (111) (clean) [69]	10	12(DMT) $\sim$ 16(JKR)	
Twofold (clean surface-with passivated probe) [6]	0.17 ± 0.03	0.18(DMT) $\sim$ 0.22(JKR)	Elastic
Tenfold (ethylene passivated) [5]	0.013 ± 0.002	$\sim$0.013(DMT)	
Tenfold (short air oxidized) [4]	0.04 ± 0.012	$\sim$0.04(DMT)	
Twofold (short air oxidized) [6]	0.045 ± 0.01	$\sim$0.045(DMT)	
Tenfold (long air oxidized)	0.02 ± 0.004	$\sim$0.02(DMT)	
Twofold (long air oxidized)	0.02 ± 0.004	$\sim$0.02(DMT)	

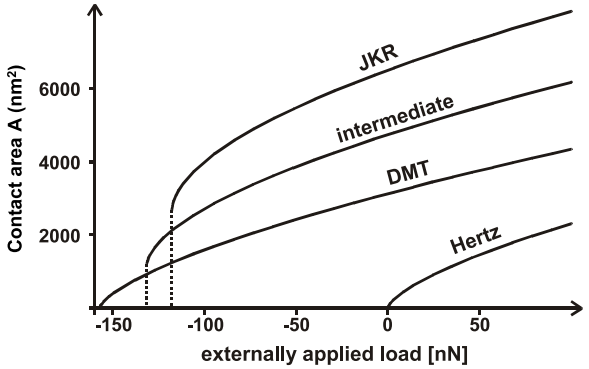

Figure 4. Plot of contact area as a function of the applied load for mechanical models of JKR, DMT, intermediate and Hertz models. R of 100 nm, K of 50 GPa, γ of 250 mJ m^{-2} and z_0 of 3 Å were used in the calculation.

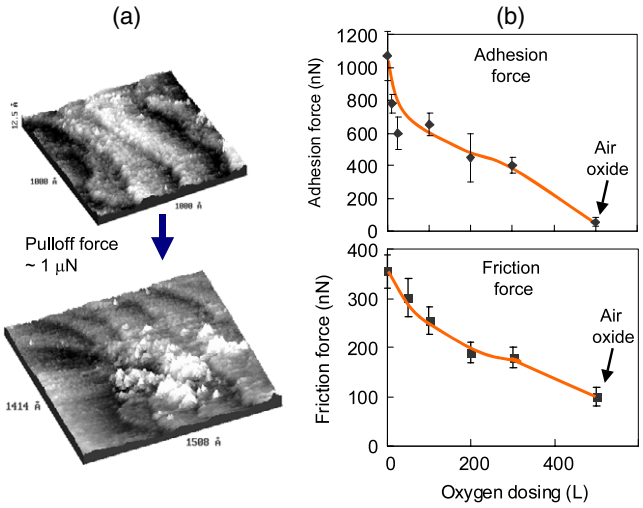

Figure 5. (a) STM images of an Al–Ni–Co quasicrystal surface before and after a force–distance experiment at the position marked by the arrow near a step edge. (b) Plot of pull-off force and friction versus oxygen uptake. (Reprinted with permission from Tribology Letters [4].)

is 120 nN (JKR) and 160 nN (DMT), which were calculated with a work of adhesion (γ) of 250 mJ m^{-2} and R of 100 nm.

5. Adhesion

Everyday experience teaches that adhesion and friction are related. Indeed, the friction coefficient between hard surfaces is classically cast as the sum of two terms, one due to the adhesion force and the other due to the mechanics of plowing [62]. In the following discussion of adhesion, it is therefore worthwhile to consider that interfaces with low adhesion would also be expected to have low friction forces.

AFM is a good probe of adhesion. Force–distance curves provide an adhesion force (see section 2.2), which can be used to derive the work of adhesion, γ, within the context of a specific model. In the JKR and DMT models, the value of γ is given by $L_c/(1.5\pi R)$ or $L_c/(2\pi R)$, respectively, where L_c is the adhesion force. In contacts between clean metals, however, plastic deformation generally occurs due to strong adhesion [62, 68]. This leads to overestimation of γ, a problem that was previously observed and addressed by Enachescu *et al* for adhesion between a WC tip and clean Pt(111) in UHV [69]. In that work, γ was measured to be 12–16 J m^{-2} [69], significantly above the range of 2–10 J m^{-2} that is expected from the range of surface energies of single elemental metals. In the presence of inelastic contributions, γ should be considered an effective value.

Measured values of adhesion force, and derived values of the work of adhesion, are given in table 1 for several types of surfaces [41]. The top two rows show results for clean surfaces of quasicrystals brought into contact with a bare AFM tip. The surfaces are high-symmetry faces of the decagonal (d-) Al–Ni–Co phase. The damage caused by the adhesion force measurement was confirmed by STM imaging of the surface before and after the contact measurement [4], as shown in figure 5(a). Note that the measured values of γ (0.4–1.1 J m^{-2} for the two surfaces combined) fall *below* the range mentioned above for typical metals (2–10 J m^{-2}), even though the former values of γ are expected to be overestimations.

The idea that γ is anomalously low for the quasicrystals is enforced by comparing it with the value for Pt(111), where the adhesion force was measured under conditions analogous to those used for the quasicrystal surfaces. The resultant work

of adhesion was at least an order of magnitude higher than the values for the quasicrystals, as shown in table 1.

The idea of low adhesion for quasicrystals was also suggested by macroscopic tribometry studies. Gellman *et al*, found that contact between a clean pair of quasicrystal surfaces did not result in measurable adhesion nor in stick–slip behavior [70], both of which are well known between clean crystalline metals [68]. (The limit of detection for adhesion in macroscopic tribometry is certainly higher (worse) than the limit of detection in an AFM experiment, so the two experimental results are not inconsistent.) Fretting tests in HV have also shown that adhesion is minimized when one counterpart is quasicrystalline [10, 20].

Thus, there exists ample support—from widely varying types of experiments—for the idea that adhesion (and hence friction) between clean, unlubricated metals is relatively low when one of the pair is a quasicrystal. This apparently extends also to certain liquid–solid interfaces. Dubois *et al* have found that the reversible work of adhesion between quasicrystals, and polar liquids such as water, is relatively low [10, 20].

Even though adhesion between the quasicrystal and tip seems relatively low, it is still high enough to make plastic deformation inevitable in FFM measurements. This problem can be circumvented by using an intervening 'buffer'. Table 1 shows several examples. (The values of γ shown in table 1 for the passivated interfaces were measured in the elastic regime, and so are not subject to the error discussed above.) For instance, the adhesion force measured for the tenfold clean surface of d-Al–Ni–Co was 0.8 μN. This decreased by as much as a factor of 40—to 0.02 μN—after oxidation, depending upon the oxidation conditions. We also found that an ethylene layer on the clean surface was a very effective passivating agent [5]. The adhesion force of the ethylene-passivated tenfold surface was only 0.013 μN at low loads, i.e. about two orders of magnitude smaller than that of the clean surface. However, both oxidation and adsorption of small molecules have the disadvantage of perturbing the atomic structure of the surface. In the case of ethylene adsorption, for example, LEED showed a loss of surface order. This defeats the goal of determining how tribological properties depend upon the atomic structure of the quasicrystal surface. A third strategy for reducing adhesion at AFM contacts, which overcomes this problem, is to chemically passivate the AFM tip, rather than the quasicrystal surface. A similar approach was utilized by Howald *et al* who imaged an Si(111) 7 × 7 reconstructed surface in contact AFM mode with a Teflon-coated tip [71]. In our experiments, we used a 16-carbon alkanethiol ($C_{16}H_{34}S$) to passivate the TiN tip [6, 41].

These strategies allowed elastic contact at low load. At high load, contact became inelastic again due to disruption of the passivating layer. For the alkanethiol-passivated tip, the adhesion force was small at low load, but increased abruptly at a pressure of about 3.3 GPa. This increase occurred when the tip pushed through the hydrocarbon layer and came into direct contact with the quasicrystal. Adhesion versus applied load was qualitatively similar for the ethylene-passivated surface, but here the transition between elastic and inelastic contact occurred at a pressure of about 4 GPa. For the unpassivated

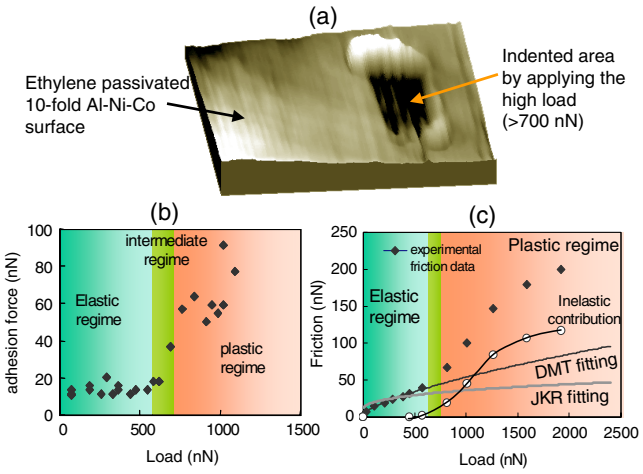

Figure 6. (a) AFM image (0.95 μm × 1.0 μm) acquired at an applied load of 150 nN. A central area, previously scanned with a load of 750 nN corresponding to a pressure of 4.1 GPa, is inelastically deformed, showing a trench with a depth of 1.0 nm. (b) Plot of adhesion force as a function of applied load. In the elastic regime, up to an applied load of 600 nN, the adhesion force is 13 nN. It increased up to 70 nN in the inelastic regime. (c) Plot of the friction force as a function of applied load. The lines are DMT and JKR fittings using the constraint of an adhesion force of 13 nN. The DMT curve fits very well with the experimental data in the elastic regime. (Reprinted figure with permission from [5]. Copyright 2005 by the American Physical Society.)

interface between a quasicrystal and AFM tip, the adhesion force was high and invariant with applied load.

These phenomena are illustrated in figure 6 for the ethylene-passivated surface. Figure 6(a) shows topographic AFM images acquired at a load of 150 nN after scanning the surface with a pressure of 4.1 GPa. The surface showed a trench in the previously scanned area with a depth of 1.0 ± 0.2 nm, with debris accumulated at the edges. Figure 6(b) shows a plot of adhesion force as a function of maximum applied load. We found that the adhesion force increased from 13 to 70 nN as the tip–surface contact changed from the elastic to inelastic regime. Likewise, the friction force increased abruptly as contact changed from elastic to inelastic. Figure 6(c) shows the friction force as a function of applied load. In the elastic regime, the DMT curve fitted very well with the experimental data, consistent with the contact of two hard materials, TiN and the passivated quasicrystal. However, above the threshold load, the experimental friction showed significant departure from the DMT curve. The abrupt increase of adhesion and friction force could be interpreted as a result of the formation of chemical bonds between the tip and the surface due to the displacement of the protective hydrocarbon molecules.

Finally, it is interesting that the value of γ on the oxidized surfaces reflects the aging effect noted in section 3. Table 1 shows that, after the quasicrystal was subjected to 'short air oxidation' (several hours in air), followed by introduction into UHV, γ was about 0.05 J m^{-2}. This value of the work of adhesion decreased after 'long air oxidation' (several months in air), to 0.02 J m^{-2}. This change presumably correlated with slow thickening of the oxide.

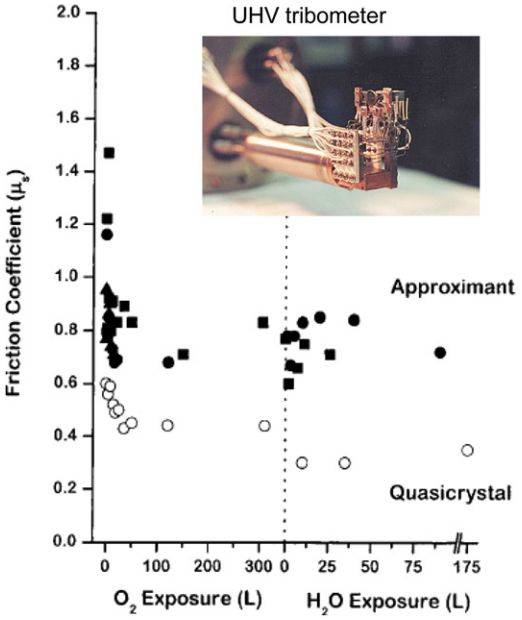

Figure 7. Friction coefficients measured between the surfaces of pairs of $Al_{48}Pd_{42}Mn_{10}$ approximants (filled symbols) and between pairs of $Al_{70}Pd_{21}Mn_9$ quasicrystals (open circles) as a function of the exposure of the surfaces to O_2 and then H_2O. The inset shows the UHV tribometer. (Reprinted with permission from the Journal of Materials Research [17].)

6. Friction on clean quasicrystals and related surfaces

6.1. Clean surfaces: inelastic contacts

The first measurements of tribological properties in UHV, where the oxide could be truly circumvented, were carried out in the laboratory of Andrew Gellman. His group employed a tribometer in which two clean surfaces of identical structure, composition and history could be brought into contact (figure 7 inset) [70]. They found that the friction coefficient between a pair of clean, single-grain fivefold Al–Pd–Mn surfaces was half of that between a pair of crystalline Al–Pd–Mn approximant surfaces [17]. Here, the Al–Pd–Mn approximant had a cubic-based structure that was a clear contrast to the icosahedral Al–Pd–Mn surface, but chemical compositions were reasonably similar.

Because the surfaces in contact were atomically clean, plastic deformation was inevitable in this experiment (cf section 5). With plastic deformation, the friction coefficient should (to first order) be proportional to the ratio of shear stress to hardness [62]. Indeed, when Mancinelli *et al* plotted friction coefficients of four pairs of clean metal surfaces in UHV as a function of hardness, they found an inverse relationship in which the quasicrystal fell smoothly on the curve [17]. This led them to suggest that hardness may be the direct cause of low friction on quasicrystals, with atomic structure playing an indirect role. However, this view has been contradicted by Dubois *et al* [20]. Those authors measured friction coefficients versus hardness for a series of samples in HV and found that quasicrystals fell significantly below the curve defined by compositionally similar materials.

Later, the group of Gellman *et al* found no variation in friction coefficient across a series of quasicrystalline-related films in the Al–Cu–Fe family, leading them to suggest that friction is not related to atomic structure [12]. However, it is possible that the tribological properties of the film were dominated by the mechanical properties of the substrate, as we will show to be the case for oxidized surfaces in section 7.2.

The expected presence of plastic deformation during friction involving a clean quasicrystal surface was first observed directly by Park *et al* [4] using FFM. As shown in figure 5(a), a pair of STM images of the tenfold Al–Ni–Co quasicrystal surface before and after an FFM measurement revealed holes and mounds, indicating wear on the surface. In this case, the friction force versus normal force could be fitted well by the JKR model, but not by DMT. The applicability of JKR was supported by the estimation of 5.15 for Tabor's parameter, using the measured adhesion force of 1.07 μN, $R = 150$ nm, $z_o = 0.2$ nm and appropriate bulk moduli. It is interesting that two hard materials (W_2C and quasicrystal) in inelastic contact followed JKR instead of DMT, since the assumptions in the JKR model are valid for soft, compliant materials in elastic contact. This is apparently a result of the strong adhesion between the clean metals in UHV since, when the interface is passivated and contact is elastic, the DMT model provides a superior fit to the friction data.

6.2. Clean surfaces: elastic contacts

In this section, we describe a comparison between friction on a quasiperiodic lattice and a periodic lattice, for an AFM tip in elastic contact with a single quasicrystal surface. This helps to clarify the roles played by hardness and adhesion, demonstrating that they alone are not sufficient to explain low friction on quasicrystals.

As mentioned in section 5, the elastic regime can be accessed with a buffer at the interface, and in this case we chose to passivate the tip with alkanethiol. A schematic of the experiment is shown in figure 8(a). Electrical measurement was used to monitor the presence of molecular layers on the probe. Before passivation the linearity of the curve indicated metallic or ohmic behavior. After passivation, the shape of the curve indicated non-metallic behavior. Figures 8(b) and (c) show AFM images taken with the passivated probe before and after the friction experiments, indicating the absence of plastic deformation.

In order to investigate the role of surface structure, it was desirable to probe periodic and aperiodic atomic arrangements nearly simultaneously. To this end, we used a twofold surface of the decagonal Al–Ni–Co phase, since it presents both periodic and aperiodic atomic arrangements. The atomically resolved STM image of the twofold Al–Ni–Co surface revealed the presence of atomic rows along the tenfold direction with an internal periodicity of 0.4 nm [72]. Along the orthogonal axis in the surface plane, the spacing between the rows followed a Fibonacci sequence with inflation symmetry. The details of the atomic structure of this twofold Al–Ni–Co surface have been presented elsewhere [72]. As shown in figure 9(a), we performed a series of experiments to explore

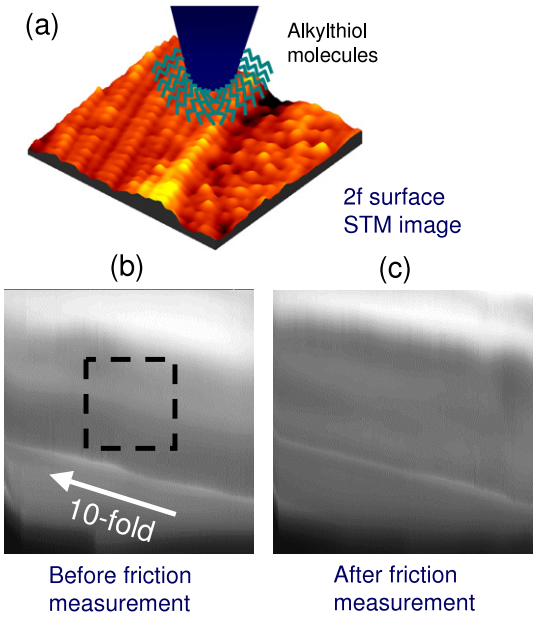

Figure 8. (a) Schematic of AFM/FFM experiment with alkylthiol molecule coated AFM probe. The image shown in (a) is a scanning tunneling microscopy image (9 nm × 9 nm) of the twofold Al–Ni–Co surface taken with the tip bias of 1.0 V and tunneling current of 0.1 nA. (b) AFM images (100 nm × 100 nm) before the friction measurement and (c) after the friction measurement, implying the absence of wear on the surface.

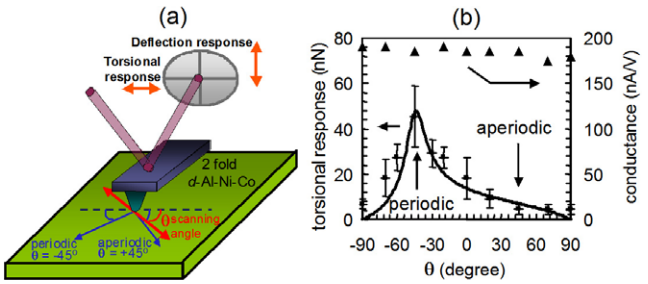

Figure 9. (a) Schematic of the rotational scanning of the AFM head used to investigate the friction anisotropy on the twofold decagonal quasicrystal. (b) Torsional response of the cantilever measured as a function of scanning angle on the twofold surface of the Al–Ni–Co decagonal quasicrystal at zero external load revealing high friction anisotropy. The solid line shows the calculated torsional response with scanning angle for an elliptical anisotropy factor (ratio of torsional response) of 8. Current at the sample bias of 1.0 V was measured at the same time as torsional response. (Reprinted figure with permission from [6]. Copyright 2006 by the American Physical Society.)

friction anisotropy as a function of scanning direction. In a conventional scanning force microscope, friction is measured by scanning the tip along the surface perpendicular to the cantilever axis. The torsional response of the cantilever is then proportional to tip–sample friction and the normal load applied to the tip–sample contact is not affected by friction. In an optical deflection AFM, a laser beam reflected off the cantilever surface close to the tip measures changes in the cantilever slope. Torsional and normal slope changes are proportional to frictional and normal forces acting on the tip, respectively. Rotating the scan angle relative to the cantilever axis introduces complications, since frictional forces now modulate the normal load applied to the contact, and the optical deflection signals show a mixed response to normal and frictional forces.

Figure 9(b) shows the torsional response of the cantilever as a function of scanning direction at an applied load of 0 nN. The overlaid curve shows the calculated torsional response as a function of rotation angle assuming an elliptical friction anisotropy ratio of 8, consistent with the measured variation of the friction in a previous, more limited experiment [8]. In figure 9(b) we also show the current measured simultaneously with torsional response. In the elastic regime, conductance is a convenient way to check for constancy of the contact area. In this experiment, the conductance was constant within 5%, indicating that the contact area was invariant with scanning angle.

Why is the friction force higher in the periodic than the quasiperiodic direction? We can begin by considering the possible explanations that were mentioned in section 1 for the low friction of quasicrystals. First, there was no oxide present in this experiment, so obviously it was not a lubricant. Second, hardness is not relevant in the elastic regime. Even if it were, hardness could be eliminated, since it is isotropic: the hardnesses along the two high-symmetry axes of the quasicrystal surface are the same to within 4% [73]. Furthermore, *any* explanation that relies upon a difference in mechanical properties is unlikely, since the conductance shows that contact area was constant with scanning angle. A third possibility is incommensurability between the probe and the surface in the aperiodic direction, which could inhibit phonon excitation and hence energy transfer [18, 19]. It may be overly simplistic to expect incommensuration to be ubiquitous; the articles by W Theis, by E Widjaja and L Marks, and by A Singh and A-P Tsai in this collection demonstrate that coherent interfaces involving quasicrystals are possible. In our experiments, the TiN tip was amorphous, and also serves as an amorphous template for the alkane thiol. Hence, differences in registry at the interface present an unlikely explanation for the anisotropy.

As mentioned in section 5, quasicrystal–metal interfaces show relatively low adhesion—as do also interfaces between quasicrystals and polar liquids. Therefore one might consider that adhesion plays a role in the observed anisotropy. However, this can be ruled out since the adhesion force is normal to the surface plane, i.e. it has no in-plane component. It can certainly contribute to friction, but it cannot be anisotropic.

Yet another cause of the anisotropy could be that the hydrocarbon chains extending from the moving tip are constrained as they sweep along the periodic rows of atoms, but less so when they move perpendicular to the rows. However, the vertical corrugation along periodic and aperiodic directions only differs by 0.01 nm—it is quite exaggerated in figure 8(a). Furthermore, a simple analogy can be made to a broom sweeping along a corrugated surface, where sweeping is expected to be easiest parallel to the direction of corrugation, which is opposite to our experimental observation.

Phasons are a special type of defect in quasicrystals and their role in friction has been discussed [15, 16]. However, relative to crystalline materials, phasons present additional channels of energy dissipation and so should serve to increase friction forces, opposite to the observation. Therefore they do not explain the anisotropy.

The two strongest options are electronic and phononic friction, i.e. energy dissipation via excitation of electron–hole pairs or phonons, respectively. Direct creation of electron–hole pairs has been invoked as a mechanism of frictional energy dissipation, and both experimental [74–76] and theoretical [77] efforts have been made to address the importance of this dissipation channel. The other mechanism is phononic friction, in which vibrations of the surface atoms are excited and subsequently damped by energy transfer to the bulk material through propagating phonon modes and in metals also by electronic excitations[4]. Phononic friction is a stronger candidate than electronic friction, since studies show that it generally dominates electronic friction [78, 79]. The excitation and propagation of phonons along the aperiodic direction could be inhibited by phonon gaps, leading to low energy dissipation. Such gaps are predicted theoretically, [80] but have not been observed experimentally [81] for quasicrystals. Either explanation is consistent with the fact that buffer layers, including chemisorbed ethylene and surface oxide, serve to reduce the friction anisotropy (see section 7.2).

Theoretical work to understand the anisotropic frictional response, using molecular dynamics simulations, is in progress [82].

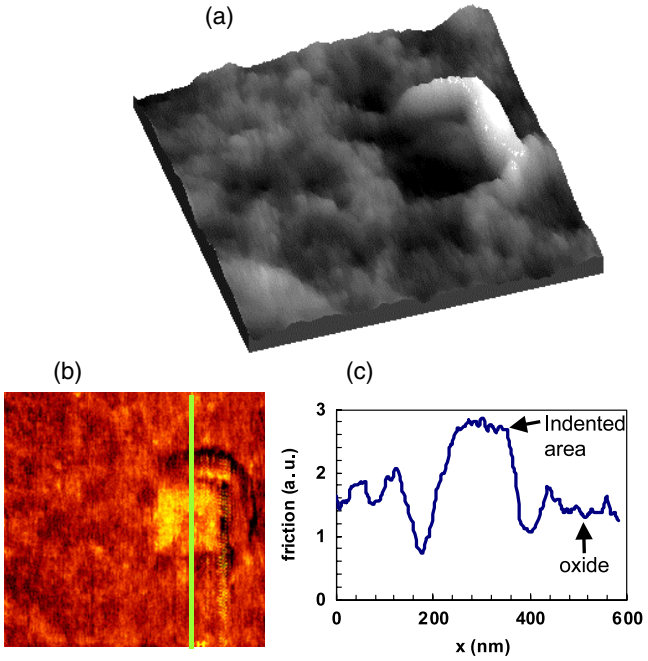

Figure 10. Images after scanning at high load on oxidized tenfold Al–Ni–Co quasicrystal surface. (a) AFM topography image (600 nm × 600 nm) that includes the scanned area, a square-shaped region 200 nm × 200 nm toward the right-hand side. (b) Friction force image after scanning at high load on oxidized surface. (c) Line profile of friction image revealing higher friction inside the indented area than inside the oxide area.

7. Comparisons of friction involving oxidized surfaces

7.1. Comparison of oxidized versus clean quasicrystal surfaces

One way to compare friction on oxidized and clean quasicrystal surfaces is to use UHV techniques. The first such effort was that of Ko *et al*, who performed tribometry in UHV as described previously (figure 7 inset) [17, 70]. They found that adsorption of oxygen or water on the fivefold surface of i-Al–Pd–Mn resulted in a decrease of friction force by about a factor of 2 [17]. Later, Mancinelli *et al* found that adsorption of oxygen or water on a crystalline approximant caused a decrease of the same magnitude [17]. These results are shown in the graph of figure 7. In these experiments contacts were probably inelastic, although that was not determined. These results showed that surface oxidation inhibits friction, but that this inhibition is not unique to quasicrystals.

Another such effort involved FFM in UHV. Figure 5(b) shows the effect of oxygen exposure on both adhesion and friction at the tenfold surface of d-Al–Ni–Co. Except for the air-oxidized sample, all measurements were made in the inelastic regime. As the oxygen exposure increased, the pull-off force decreased from 1070 nN on the clean surface to 450 nN after an exposure of 200 L and remained saturated thereafter up to 10^3 L. The air-oxidized surface, however, showed a much smaller pull-off force of 55 nN, presumably reflecting the fact that air oxidation resulted in a much thicker oxide [52]. This is consistent with the adhesion results presented already in section 5. Figure 5(b) also shows the friction force as a function of oxygen exposure at an applied load of 1000 nN. Friction forces decreased rapidly in the early stages of oxygen adsorption (0–100 L) and became saturated after a 200 L dose. This is entirely consistent with the previous tribological measurements on the fivefold i-Al–Pd–Mn quasicrystal surfaces [17, 70]. Because the air-oxidized sample was measured in elastic contact, unlike the other data points, it cannot be compared directly, but it is included in the figure for completeness.

In yet another type of comparison between clean and oxidized quasicrystal surfaces, we took advantage of the wear that occurs on an air-oxidized surface upon scanning at high load (>1000 nN). Figure 10 shows the AFM image of a scanned, worn area (200 nm × 200 nm) contained within a larger image. The worn area was indented, with a depth of 6 nm and debris near the hole. Since the typical thickness of the air oxide on quasicrystal surfaces is 2–6 nm [52, 55, 83], we can assume that the fresh quasicrystal surface was exposed inside the indented area. The experiment was performed in UHV, so there is no re-growth of the surface oxide after its removal. As shown by figures 10(b) and (c), the friction force was higher—by about a factor of 2—inside the indented area than in the surrounding region. Therefore, we conclude that the bare quasicrystal surface shows higher friction force than

[4] Many authors avoid referring to quasicrystals as metals, although we do so in this paper for convenience.

the oxide by a factor of 2. This result is also consistent with the other studies cited in this section.

Similar AFM/FFM studies were performed by Drobek *et al* [7], who also measured higher friction force inside a depressed region formed by scanning at high load on tenfold d-Al–Ni–Co. Drobek's AFM work was, however, performed in air. Thus, the oxide must have re-formed after wear, but it was almost certainly thinner than the surrounding, unperturbed oxide (cf section 5). Thus, this result can be explained by higher adhesion, and therefore higher friction, on the thinner oxide inside the depression.

The above reports deal with plastic contacts. There is evidence that oxygen also lowers the friction force, relative to the clean surface, when contact is elastic. In our AFM/FFM experiments with a passivated tip and twofold d-Al–Ni–Co, we found not only that the friction anisotropy disappeared upon oxidation as will be discussed in section 7.2, but also that the magnitude of the friction force dropped by about a factor of 1.5 relative to friction in the clean quasiperiodic (periodic) direction at a total load of 50 nN [8].

Dubois *et al* have also reported that the coefficient of friction on quasicrystals and related crystalline alloys generally drops when a small amount of oxygen is introduced during tribometry in HV [20], although a conflicting report also exists. In the latter experiment, air was introduced during HV tribometry of a quasicrystal, and caused an increase in the friction coefficient [11]. The reason for the discrepancy is not clear.

In summary, several studies have shown that surface oxidation serves to reduce the friction coefficient or friction force at a quasicrystal surface. This effect of oxidation is not unique to quasicrystals. A reduction is observed regardless of whether contact is elastic or inelastic, provided that the oxide remains intact during sliding. The reduction correlates with the lower adhesion.

7.2. *Comparison of quasiperiodic versus periodic crystals*

Recently, we measured friction and adhesion on twofold and fivefold icosahedral Al–Pd–Mn surfaces, on twofold and tenfold Al–Ni–Co decagonal surfaces, on an Al–Pd–Mn approximant and on a polycrystalline aluminum substrate. Each substrate was covered with aluminum oxide. The friction measurements were performed in the elastic regime, which was confirmed by imaging the surface after measurement. Under these conditions, we found that the friction coefficient measured on the polycrystalline aluminum substrate is higher than on the other materials by a factor of 2.

It is appropriate to give some experimental details, since these results have not been reported previously. Five single-grain samples were examined: twofold and fivefold surfaces of i-Al–Pd–Mn quasicrystals, a pseudo-tenfold surface of the ξ'-Al–Pd–Mn approximant, and twofold and tenfold surfaces of d-Al–Ni–Co. A sixth sample, polycrystalline Al, was obtained by depositing an aluminum film (thickness of 500 nm) onto an Si(100) wafer. Prior to AFM/FFM measurements, the samples were oxidized in ambient air at room temperature. We expect that the 500 nm film of Al reflects the frictional properties

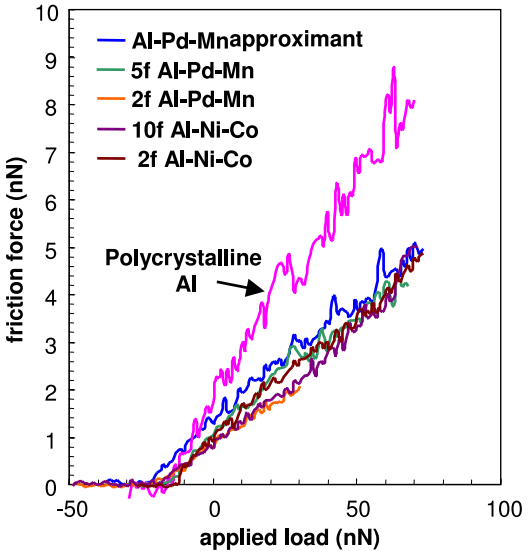

Figure 11. Friction as a function of the applied load measured on various Al-based quasicrystal and approximant surfaces and polycrystalline Al film.

of a bulk Al surface because the Young's modulus of bulk Al is 70 GPa, similar to the value of the thin film [84], and furthermore the chemical nature of aluminum oxide on the aluminum film should be the same as that on bulk Al.

For quantitative measurements of friction and adhesion forces, it is crucial to have constant cantilever parameters, such as spring constant and tip radius. For this reason, we used the same cantilever for the whole series of friction measurements. To check whether or not the radius of the tip remained constant, friction was measured as a function of load on a reference sample before and after each set of friction measurements. The same friction values and lateral resolution were measured on the reference sample, confirming the same spring constant and tip radius throughout the experiments.

Figure 11 shows the friction measured on the different surfaces as a function of applied load. As shown in figure 11, the friction measured on the polycrystalline aluminum was higher than that on the quasicrystals and approximant by about a factor of 2. We did not see any change on any surface after the friction measurements, thus indicating the absence of wear. Adhesion forces of the samples were ∼17–25 nN. In table 2, the values of adhesion force, surface roughness, work of adhesion (using a tip radius of 100 nm) and friction coefficient for different samples are listed. It can be seen that the friction coefficient does not correlate with any of these parameters.

The variation of friction force on different surfaces can be associated, instead, with the variation of Young's modulus (K). This can be rationalized as follows. In the case of mechanical contacts between hard materials, we can use the DMT model. The friction force (F_f) is given by

$$F_f = \tau A = \tau\pi \left(\frac{R^{2/3}}{K^{2/3}}\right) \times (L + L_c)^{2/3} \qquad (3)$$

where A is the contact area, L is applied load and τ is the critical shear strength defined as the shear force per unit area

Table 2. Adhesion force, work of adhesion, friction coefficient and surface roughness measured on surfaces of quasicrystals, an approximant and a polycrystalline Al sample. Work of adhesion was estimated by using the DMT model with a tip radius of 100 nm.

	Adhesion (nN)	Friction coefficient	Surface roughness (Å)	Work of adhesion (mJ m^{-2})
Approximant Al–Pd–Mn	22 ± 7	0.052 ± 0.03	2.5	35
Fivefold i-Al–Pd–Mn	20 ± 5	0.050 ± 0.03	3.1	32
Twofold i-Al–Pd–Mn	20 ± 5	0.046 ± 0.02	3.0	32
Twofold d-Al–Ni–Co	15 ± 5	0.049 ± 0.04	3.5	24
Tenfold d-Al–Ni–Co	17 ± 5	0.049 ± 0.03	3.3	27
Polycrystalline Al	18 ± 4	0.092 ± 0.06	3.8	28

(or per atom) required to shear the interface. Other parameters have been defined in section 4. Because the contact area is proportional to $1/K^{2/3}$, variation of combined Young's modulus, and Poisson's ratio, changes the contact area, and thus friction force. In our case, the Poisson ratios of the six tested surfaces are in the range of 0.33–0.4, yielding $1 - \upsilon^2 =$ 0.84–0.88. Therefore the change of K due to variation in Poisson's ratio is only 5%.

To a good approximation, then, the variation of friction forces is mainly associated with Young's modulus of the tested samples. The Al surface had the lowest Young's modulus (∼50–70 GPa [84]) out of the six tested surfaces. Most quasicrystalline materials have much higher moduli, ranging from 150 to 200 GPa. For example, Young's modulus of tenfold Al–Ni–Co is 177 GPa [85], twofold Al–Ni–Co is 195 GPa [73] and i-Al–Pd–Mn is 190 GPa [86]. The combined elastic modulus (K) between Al and TiN is 70–90 GPa, lower than the 210–230 GPa for quasicrystals and TiN, resulting in the larger contact area for Al surfaces. These were calculated with $E_{\mathrm{TiN}} = 600$ GPa, $\nu_{\mathrm{TiN}} = 0.25$, $\nu_{\mathrm{QC}} = 0.38$ and $\nu_{\mathrm{Al}} = 0.33$. If we assume the shear strength is uniform for these samples, because all the surfaces were covered with aluminum oxide with identical surface chemistry, we can conclude that the frictional responses of these six surfaces were mainly determined by the elastic properties of the substrate beneath the oxide layer rather than on its detailed atomic structure.

The dependence of friction coefficient on Young's modulus was recently studied with FFM by Riedo and Brune on CrN, diamond and diamond-like-carbon thin films [87]. In those studies also, it was found that the nanoscopic friction coefficient is directly linked to Young's modulus, if contact is elastic and if the materials have similar Poisson's ratios.

There is further support for the idea that friction force does not depend directly on bulk atomic structure, when the surface is oxidized and if contact is elastic. This comes from our measurements of friction anisotropy on the oxidized twofold surface of d-Al–Ni–Co. As discussed in section 6.2, friction force is highly anisotropic when the quasicrystal surface is clean, showing a strong sensitivity to quasiperiodic versus periodic order. However, when the surface is oxidized, the anisotropy is quenched, indicating that the atomic structure of the metal no longer exerts an influence [6, 8].

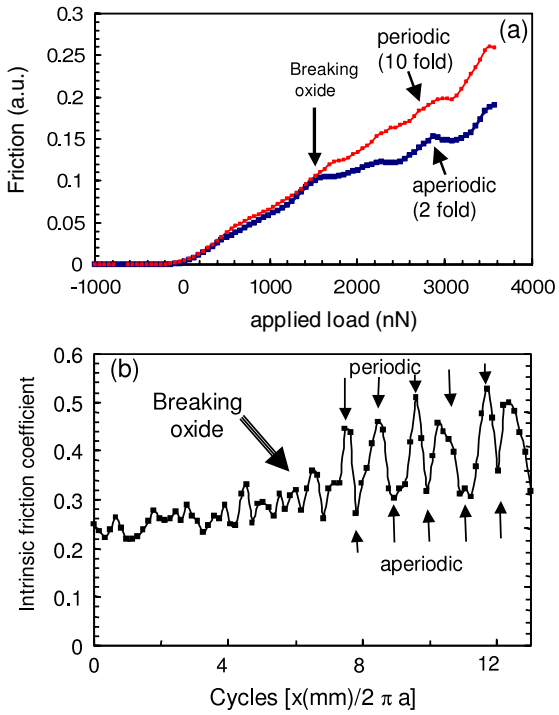

Figure 12. (a) Friction force measured with the atomic force microscope as a function of the applied load. Friction along the periodic (tenfold) direction is higher than that along the aperiodic (twofold) direction after the oxide layer is broken when the load reached 1.5 μN. (b) Friction coefficient measured with pin-on-disc. After the pin penetrates the oxide a friction anisotropy was observed, with high friction along the periodic quasicrystal direction and low friction along the aperiodic direction.

8. Frictional anisotropy under other conditions

Work presented in the preceding sections showed that a strong friction anisotropy is observed in FFM experiments, for elastic contacts with the clean twofold surface of d-Al-Ni-Co. However, can a link be made between the friction anisotropy observed under these rather esoteric conditions, and the low friction observed on quasicrystals under macroscopic tribological conditions? If so, friction anisotropy should still be observed on the twofold decagonal surface in the latter case, provided that the quasiperiodicity of the metal is neither obscured by an oxide nor disrupted excessively by the contact.

To address the issue, we performed a tribological study on this surface using both an AFM/FFM and a pin-on-disc tribometer [88]. In both cases, the surface was initially covered by oxide from air exposure, but as wear proceeded the oxide was destroyed. The measurements were done in vacuum, and the oxide could not re-form on the timescale of the measurements.

The friction force measured with AFM/FFM along each of the two crystallographic directions (twofold and tenfold) was measured as a function of increasing load and the results are shown in figure 12(a). In these experiments, the AFM probe scanned repetitively over the same vertical line, while load was varied. Figure 12(a) shows no noticeable difference in

friction force between periodic and quasiperiodic directions, up to 1.5 μN. This isotropic response can be attributed to the fact that the aluminum oxide was amorphous, and that it remained intact at low loads. The two friction force curves diverge above 1.5 μN. This is because the oxide film ruptured at this load, as confirmed by the AFM images, acquired before and after one set of friction measurements. Therefore the AFM tip made contact with the quasicrystalline metal at the higher applied loads, giving rise to the observed friction anisotropy between periodic and quasiperiodic directions. The magnitude of the anisotropy, defined as the ratio of the friction forces along tenfold to twofold directions, was 1.2–1.4.

The friction force signal and the position of the pin were simultaneously measured on the oxidized Al–Ni–Co decagonal surface with pin-on-disc in HV. As shown in figure 12(b), for the first few tens of rotations no wear was detected within experimental accuracy. After many more rotations, however, abrasion of one or both materials by a fraction of a micrometer was detected. The plot clearly reveals the friction anisotropy of the twofold decagonal surface in the regime where irreversible removal of the oxide layer occurs. Assuming that the highest friction is exhibited along the tenfold axis, the friction coefficient along the periodic direction is 0.45 ± 0.06. This is higher than that along the aperiodic direction (0.30 ± 0.05) by a factor of 1.5, almost exactly the same as the value measured with FFM.

From the results presented in this section we can conclude that friction anisotropy is a property that appears not only in nanoscale systems but also in larger scale systems at the micrometer scale, since AFM and pin-on-disc explore vastly different load and length scales. The different length scales are demonstrated by calculating the trace width (TW) of the wear track. In the DMT model, $\mathrm{TW} = 2(L \times R/K)^{1/3}$, where L is the applied load, and other parameters have been defined previously. The trace width for AFM measurements is $\mathrm{TW_{AFM}} = 2(L \times R/K)^{1/3} = 21$ nm for $R = 100$ nm and $L = 2$ μN. In the case of the pin-on-disc measurement, for AISI (SAE) 52 100 steel, $E = 206$ GPa and $\nu = 0.3$ [89], yielding $K = 153$ GPa. In that case, with $R = 6$ mm, $\mathrm{TW_{pin\text{-}on\text{-}disc}} = 68$ μm. Therefore, these two measurements represent tribological results at two different length scales, nanometer and macroscopic.

In a somewhat similar experiment, Wittman *et al* pointed out an anisotropy of friction probed in air using a scratch test experiment (24). The anisotropy for a spherical diamond indenter of small (but unspecified) radius was 1.3 for scratching parallel (high friction) or perpendicular (low friction) to the periodic axis. This is surprisingly close to the values measured with AFM/FFM in UHV (1.2–1.4) and with pin-on-disc in HV (1.5).

These results demonstrate that the low friction measured on quasicrystalline materials is associated with the quasicrystalline atomic structure, even when friction is accompanied by irreversible damage. However, the magnitude of the friction anisotropy is much lower in the presence of damage, suggesting that the friction forces directly associated with wear are not dependent on quasiperiodic order.

9. Friction, adhesion and friction anisotropy: toward a unified view?

From the numerous comparisons made, and experimental results presented in this paper, let us construct some generalities and make some speculations.

First, there is abundant evidence that low adhesion and low friction are both characteristic of quasicrystals, and are directly related to the quasiperiodic atomic structure. It is therefore tempting to attribute low friction (at least in part) to low adhesion. Second, there is strong evidence of a friction anisotropy on quasicrystal surfaces having anisotropic atomic structure. In section 6.2 we argued that this friction anisotropy *cannot* be due to adhesion, but rather is probably due to anisotropic phonon excitation cross sections at the sliding interface. Hence, it would appear that two *different* fundamental factors contribute to low friction at quasicrystal surfaces: low adhesion (mainly an electronic effect) and inefficient phonon excitation (a dynamic effect).

This hypothesis is supported by the fact that it can explain an apparent contradiction that arises in the comparison of friction on clean versus oxidized surfaces. On the one hand, friction forces are generally higher on clean quasicrystal surfaces than on oxidized surfaces. This can be explained by lower adhesion on the oxidized surfaces. On the other hand, the friction anisotropy disappears when the clean surface is oxidized. This is difficult to reconcile unless the source of the anisotropy is different from, and independent of, the first case.

The relative importance of these two factors will depend upon the conditions of sliding and the type of comparison that is being made. In comparisons among clean metals, or between metals where the clean surface is exposed by wear, the dynamic factor will contribute most in elastic contacts; adhesion must play an increasing role in inelastic contacts. In comparisons between clean and oxidized surfaces, adhesion forces dominate. In comparisons among oxidized surfaces, adhesion and friction depend upon the oxide thickness. If the oxide is thick, such that adhesion forces are constant, this type of comparison reveals that friction also depends upon the mechanical properties of the underlying metal.

Of course, all of the conditions discussed in this paper correspond to very low (even zero) rates of wear, and most of the experiments are carried out in vacuum. Under more realistic conditions, other mechanisms such as third-body lubrication by the oxide, or phase transitions in the wear track, may be important as well.

10. Conclusions

The principles that emerge from the work presented in this paper can be summarized as follows, for the Al-based quasicrystals Al–Pd–Mn and Al–Ni–Co, and related materials.

(1) The clean quasicrystal surface exhibits unavoidable adhesion when it comes into contact with metallic nitride or carbide on an AFM tip, and probably with other metals as well. Strong adhesion is well known when clean metal surfaces come into contact. However, the quasicrystal is associated with lower adhesion than a regular crystalline

metal. This is based upon UHV-AFM, and compares well with conclusions drawn from UHV tribometry and HV fretting measurements.

(2) Low adhesion and elastic contact at low loads, between quasicrystals and other metals, can be achieved with the insertion of an intervening molecular or oxidic buffer, based upon UHV-AFM/FFM. If the buffer is an oxide prepared in air, adhesion depends upon the aging of the oxide, with longer aging corresponding to thicker oxides and lower adhesion.

(3) In elastic contact with a clean quasicrystal (achieved with a passivated AFM tip), friction force depends strongly upon whether the atomic arrangement is periodic or quasiperiodic. High friction anisotropy was revealed on the twofold Al–Ni–Co surface, with friction being 8× higher along the periodic direction than along the aperiodic direction. The explanation for this can be narrowed down to inefficient elementary excitations at the interface, most probably inefficient phonon excitation.

(4) The presence of an oxide serves to reduce friction on initially clean quasicrystals and related crystals, for plastic and elastic contacts alike, at least as long as the oxide remains intact. This can be attributed to lower adhesion at the interface with the oxide than with the clean metal. This is based upon UHV-AFM/FFM, and compares well with conclusions drawn from tribometry experiments in both UHV and HV. An AFM/FFM experiment in air may support the conclusion that friction is higher at a thinner (less aged) oxide, which would parallel the adhesion trends.

(5) On the oxidized surface and in the elastic regime, friction is dominated by the bulk properties of the metal beneath the oxide, and is not sensitive to whether the metal is quasiperiodic or periodic. In a comparison between several quasicrystalline materials, an approximant and polycrystalline Al, the latter exhibited the highest friction due to its lower Young's modulus and consequent higher contact area. Furthermore, friction forces are isotropic on a twofold d-Al–Ni–Co surface after oxidation. These conclusions are based on UHV-AFM/FFM of air-oxidized samples.

(6) The clean twofold surface of d-Al–Ni–Co (which is revealed after wear of an overlying oxide layer) reveals a friction anisotropy of ∼1.4 in the inelastic regime. This is smaller than the anisotropy of 8 observed in the elastic regime, implying that the low friction of the quasicrystal surface is obscured by inelastic deformation and wear. These conclusions are based on both UHV-AFM/FFM and HV tribometry.

(7) Overall, the good agreement between nanoscopic and macroscopic friction and adhesion measurements indicates that both approaches provide excellent insight into common, fundamental origins of tribology.

Finally, we have suggested a general framework for friction, adhesion and dynamic effects at quasicrystal surfaces, which explains the relative importance of these factors when comparisons are made between different types of samples and under different mechanical regimes of contact.

Acknowledgments

This work was supported by the Director, Office of Energy Research, Office of Basic Energy Sciences, Materials Sciences Division, of the US Department of Energy through the Ames Laboratory, contract no. W-405-Eng-82, and through the Lawrence Berkeley National Laboratory, contract no. DE-AC02-05CH11231. We thank Miquel Salmeron, Frank Ogletree and Cynthia Jenks for valuable discussions. We thank Vincent Fournée and David Rabson for helpful and insightful comments. We thank P C Canfield and his group for providing some of the single-grain samples of the quasicrystals.

References

[1] Dubois J-M 2005 *Useful Quasicrystals* (Singapore: World Scientific)
[2] Dubois J M, Kang S S and Vonstebut J 1991 *J. Mater. Sci. Lett.* **10** 537–41
[3] Kang S S, Dubois J M and von Stebut J 1993 *J. Mater. Res.* **8** 2471
[4] Park J Y, Ogletree D F, Salmeron M, Jenks C J and Thiel P A 2004 *Tribol. Lett.* **17** 629–36
[5] Park J Y, Ogletree D F, Salmeron M, Ribeiro R A, Canfield P, Jenks C J and Thiel P A 2005 *Phys. Rev.* B **71** 144203
[6] Park J Y, Ogletree D F, Salmeron M, Ribeiro R A, Canfield P C, Jenks C J and Thiel P A 2006 *Phys. Rev.* B **74** 024203
[7] Drobek T and Heckl W M 2000 *Mater. Sci. Eng.* A **294** 878–81
[8] Park J Y, Ogletree D F, Salmeron M, Ribeiro R A, Canfield P C, Jenks C J and Thiel P A 2005 *Science* **309** 1354–6
[9] Duckham A, Shechtman D and Grushko B 2001 *Mater. Res. Soc. Symp. Proc.* **643** K8.1.1–6
[10] Dubois J M, Brunet P, Costin W and Merstallinger A 2004 *J. Non-Cryst. Solids* **334** 475–80
[11] Dubois J M, Fournée V and Belin-Ferrée E 2004 *Quasicrystals 2003—Preparation, Properties and Applications* ed E Belin-Ferre *et al* (Warrendale, PA: Materials Research Society) pp 287–98
[12] Rampulla D M, Mancinelli C M, Brunell I F and Gellman A J 2005 *Langmuir* **21** 4547–53
[13] Singer I L, Dubois J M, Soro J M, Rouxel D and von Stebut J 1998 *(ICQ6): Proc. 6th Int. Conf. on Quasicrystals* ed S Takeuchi and T Fujiwara (Singapore: World Scientific) pp 769–72
[14] Dong C, Wu J, Zhang L, Dubois J-M, Brunet P, Zhou Q, Wang D and Zhang H 2001 *Mater. Res. Soc. Symp. Proc.* **643** K7.5.1–11
[15] Janssen T 2004 *J. Non-Cryst. Solids* **334/335** 471–4
[16] Janssen T, Radulescu O and Rubtsov A N 2002 *Eur. Phys. J.* B **29** 85–95
[17] Mancinelli C, Jenks C J, Thiel P A and Gellman A J 2003 *J. Mater. Res.* **18** 1447–56
[18] Lancon F, Penisson J M and Dahmen U 2000 *Europhys. Lett.* **49** 603–9
[19] Vanossi A, Röder J, Bishop A R and Bortolani V 2000 *Phys. Rev.* E **63** 017203
[20] Dubois J M, De Weerd M C, Brenner J, Sales M, Mozdzen G, Merstallinger A and Belin-Ferre E 2006 *Phil. Mag.* **86** 797–805
[21] Belin-Ferre E and Dubois J-M 2007 *Mater. Sci. Eng.* A **A449–A451** 971–4
[22] Ding Y, Northwood D O and Alpas A T 1997 *Surf. Coat. Technol.* **96** 140–7

[23] Dong C, Zhang L-M, Zhou Q-G, Zhang H-C, Dubois J-M, Zhang Q-H, Fu Y-C, He F-Z and Ge F 1999 *Bull. Mater. Sci.* **22** 465–72
[24] Fehrenbacher L, Zabinski J S, Phillips B S, Daniels M J, King D, Ketola K S and Bilello J C 2004 *Tribol. Lett.* **17** 435–43
[25] Feng L P, Shao T M, Jin Y J, Fleury E, Kim D H and Chen D R 2005 *J. Non-Cryst. Solids* **351** 280–7
[26] Milman Y V, Lotsko D V, Dub S N, Ustinov A I, Polishchuk S S and Ulshin S V 2007 *Surf. Coat. Technol.* **201** 5937–43
[27] Phillips B S and Zabinski J S 2003 *Tribol. Lett.* **15** 57–64
[28] Phillips B S and Zabinski J S 2004 *Tribol. Lett.* **17** 429–34
[29] von Stebut J, Soro J M, Plaindoux P and Dubois J M 1997 *New Horizon Quasicrystals* ed A I Goldman *et al* (Singapore: World Scientific) pp 248–55
[30] Zhou C G, Cai F, Kong J, Gong S K and Xu H B 2004 *Surf. Coat. Technol.* **187** 225–9
[31] Zhou X Y, Li P Y, Luo J M, Qian S Q and Tong J H 2004 *J. Mater. Sci. Technol.* **20** 709–13
[32] Mate C M, McClelland G M, Erlandsson R and Chiang S 1987 *Phys. Rev. Lett.* **59** 1942–5
[33] Carpick R W and Salmeron M 1997 *Chem. Rev.* **97** 1163–94
[34] Gnecco E, Bennewitz R, Gyalog T and Meyer E 2001 *J. Phys.: Condens. Matter* **13** R619–42
[35] Park J Y, Phaneuf R J, Ogletree D F and Salmeron M 2005 *Appl. Phys. Lett.* **86** 172105
[36] Park J Y, Sacha G M, Enachescu M, Ogletree D F, Ribeiro R A, Canfield P C, Jenks C J, Thiel P A, Saenz J J and Salmeron M 2005 *Phys. Rev. Lett.* **95** 136802
[37] Bhushan B, Israelachvili J N and Landman U 1995 *Nature* **374** 607–16
[38] Israelachvili J N and Adams G E 1978 *J. Chem. Soc. Faraday Trans.* I **74** 975
[39] Krim J 2007 *Nano Today* **2** 38–43
[40] Liu Y, Erdemir A and Meletis E I 1996 *Surf. Coat. Technol.* **82** 48–56
[41] Park J Y, Ogletree D F, Salmeron M, Ribeiro R A, Canfield P C, Jenks C J and Thiel P A 2006 *Phil. Mag.* **86** 945–50
[42] Oshea S J, Welland M E and Wong T M H 1993 *Ultramicroscopy* **52** 55–64
[43] Sader J E, Chon J W M and Mulvaney P 1999 *Rev. Sci. Instrum.* **70** 3967–9
[44] Ogletree D F, Carpick R W and Salmeron M 1996 *Rev. Sci. Instrum.* **67** 3298–306
[45] Thiel P A, Jenks C J and Goldman A I 1999 *Physical Properties of Quasicrystals* ed Z Stadnik (Berlin: Springer) pp 327–59
[46] McGrath R, Ledieu J, Cox E J and Diehl R D 2002 *J. Phys.: Condens. Matter* **14** R119–44
[47] Fournée V and Thiel P A 2005 *J. Phys. D: Appl. Phys.* **38** R83–106
[48] Sharma H R, Shimoda M and Tsai A P 2007 *Adv. Phys.* **56** 403–64
[49] Chang S L, Chin W B, Zhang C M, Jenks C J and Thiel P A 1995 *Surf. Sci.* **337** 135–46
[50] Longchamp J N, Burkardt S, Erbudak M and Weisskopf Y 2007 *Phys. Rev.* B **76** 094203/094201–5
[51] Kang S-S and Dubois J-M 1995 *J. Mater. Res.* **10** 1071–4
[52] Chang S-L, Anderegg J W and Thiel P A 1996 *J. Non-Cryst. Solids* **195** 95–101
[53] Pinhero P J, Chang S-L, Anderegg J W and Thiel P A 1997 *Phil. Mag.* B **75** 271–81
[54] Gu T, Goldman A I, Pinhero P and Delaney D 1997 *New Horizons in Quasicrystals: Research and Applications* ed A I Goldman *et al* (Singapore: World Scientific) pp 165–8
[55] Pinhero P J, Anderegg J W, Sordelet D J, Besser M F and Thiel P A 1999 *Phil. Mag.* B **79** 91–110
[56] Demange V, Anderegg J W, Ghanbaja J, Machizaud F, Sordelet D J, Besser M F, Thiel P A and Dubois J M 2001 *Appl. Surf. Sci.* **173** 327–38
[57] Alexander M R, Thompson G E and Beamson G 2000 *Surf. Interface Anal.* **29** 468–77
[58] Alexander M R, Thompson G E, Zhou X, Beamson B and Fairley N 2002 *Surf. Interface Anal.* **34** 485–9
[59] Veys D, Weisbecker P, Fournée V, Domenichini B, Weber S, Rapin C and Dubois J M 2004 *Mater. Res. Soc. Symp. Proc.* **805** LL8.8.1
[60] Rouxel D, Gavatz M, Pigeat P and Weber B 1997 Auger electron microprobe analysis of surface of $Al_{62}Cu_{25.5}Fe_{12.5}$ quasicrystal. First steps of oxidation *New Horizon Quasicrystals* ed A I Goldman *et al* (Singapore: World Scientific) pp 173–80
[61] Gil-Gavatz M, Rouxel D, Pigeat P, Weber B and Dubois J-M 2000 *Phil. Mag.* A **80** 2083–97
[62] Hutchings I M 1992 *Tribology: Friction and Wear of Engineering Materials* (Boca Raton, FL: CRC Press)
[63] Derjaguin B V, Muller V M and Toporov Y P 1975 *J. Colloid Interface Sci.* **53** 314–26
[64] Enachescu M, van den Oetelaar R J A, Carpick R W, Ogletree D F, Flipse C F J and Salmeron M 1998 *Phys. Rev. Lett.* **81** 1877–80
[65] Johnson K L, Kendall K and Roberts A D 1971 *Proc. R. Soc.* A **324** 301
[66] Carpick R W, Ogletree D F and Salmeron M 1999 *J. Colloid Interface Sci.* **211** 395–400
[67] Schwarz U D 2003 *J. Colloid Interface Sci.* **261** 99–106
[68] Buckley D H 1981 *Surface Effects in Adhesion, Friction, Lubrication and Wear* (Amsterdam: Elsevier)
[69] Enachescu M, Carpick R W, Ogletree D F and Salmeron M 2004 *J. Appl. Phys.* **95** 7694
[70] Ko J S, Gellman A J, Lograsso T A, Jenks C J and Thiel P A 1999 *Surf. Sci.* **423** 243–55
[71] Howald L, Luthi R, Meyer E and Guntherodt H J 1995 *Phys. Rev.* B **51** 5484–7
[72] Park J Y, Ogletree D F, Salmeron M, Ribeiro R A, Canfield P C, Jenks C J and Thiel P A 2005 *Phys. Rev.* B **72** 220201
[73] Paufler P and Wolf B 2003 *Deformation of Quasicrystals by Indentation Quasicrystals: Structure and Physical Properties* ed Hans-Rainer Trebin (Weinheim: Wiley–VCH) p 501
[74] Dayo A, Alnasrallah W and Krim J 1998 *Phys. Rev. Lett.* **80** 1690–3
[75] Witte G, Weiss K, Jakob P, Braun J, Kostov K L and Woll C 1998 *Phys. Rev. Lett.* **80** 121–4
[76] Park J Y, Ogletree D F, Thiel P A and Salmeron M 2006 *Science* **313** 186
[77] Persson B N J 1998 *Sliding Friction: Physical Principles and Applications* (Berlin: Springer)
[78] Coffey T and Krim J 2005 *Phys. Rev. Lett.* **95** 076101
[79] Tomassone M S, Sokoloff J B, Widom A and Krim J 1997 *Phys. Rev. Lett.* **79** 4798
[80] Theis W, Sharma H R, Franke K J and Rieder K H 2004 *Prog. Surf. Sci.* **75** 227–36
[81] Dugain F, De Boissieu M, Shibata K, Currat R, Sato T J, Kortan A R, Suck J-B, Hradil K, Frey F and Tsai A P 1999 *Eur. Phys. J.* B **7** 513–6
[82] Harper H M and Rabson D A 2008 unpublished
[83] Rouxel D and Pigeat P 2006 *Prog. Surf. Sci.* **81** 488–514
[84] Chinmulgund M, Inturi R B and Barnard J A 1995 *Thin Solid Films* **270** 260–3
[85] Li X, Zhang L and Gao H 2004 *J. Phys. D: Appl. Phys.* **37** 753–7
[86] Wolf B and Paufler P 1999 *Phys. Status Solidi* a **172** 341–61
[87] Riedo E and Brune H 2003 *Appl. Phys. Lett.* **83** 1986–8
[88] Park J Y, Ogletree D F, Salmeron M, Jenks C J, Thiel P A, Brenner J and Dubois J M 2008 *J. Mater. Res.* **23** 1488–93
[89] Borodich F M, Harris S J, Keer L M and Cooper C V 2004 *Surf. Coat. Technol.* **179** 78–82